

Target-driven Self-Distillation for Partial Observed Trajectories Forecasting

Pengfei Zhu^{1*}, Peng Shu^{1*}, Mengshi Qi^{1†}, Liang Liu¹ and Huadong Ma¹

¹Beijing Key Laboratory of Intelligent Telecommunications Software and Multimedia,
Beijing University of Posts and Telecommunications, Beijing, 100876
{zhupengfei2000, shup, qms, liangliu, mhd}@bupt.edu.cn,

Abstract

Accurate prediction of future trajectories of traffic agents is essential for ensuring safe autonomous driving. However, partially observed trajectories can significantly degrade the performance of even state-of-the-art models. Previous approaches often rely on knowledge distillation to transfer features from fully observed trajectories to partially observed ones. This involves firstly training a fully observed model and then using a distillation process to create the final model. While effective, they require multi-stage training, making the training process very expensive. Moreover, knowledge distillation can lead to a performance degradation of the model. In this paper, we introduce a **Target-driven Self-Distillation method (TSD)** for motion forecasting. Our method leverages predicted accurate targets to guide the model in making predictions under partial observation conditions. By employing self-distillation, the model learns from the feature distributions of both fully observed and partially observed trajectories during a single end-to-end training process. This enhances the model’s ability to predict motion accurately in both fully observed and partially observed scenarios. We evaluate our method on multiple datasets and state-of-the-art motion forecasting models. Extensive experimental results demonstrate that our approach achieves significant performance improvements in both settings. To facilitate further research, we will release our code and model checkpoints.

1 Introduction

For the autonomous driving system, predicting the trajectory of surrounding agents within the next few seconds is a crucial and challenging task. Accurate motion forecasting can enhance the safety of autonomous driving by promoting precise path planning and guiding the agents to follow safe routes, thereby rendering substantial support for ego-vehicle trajectory planning within the autonomous driving

pipeline [Jia *et al.*, 2023; Hu *et al.*, 2023; Wu *et al.*, 2022], as well as aiding in robot navigation [Huang *et al.*, 2023; Chen *et al.*, 2019] and tracking [Cui *et al.*, 2022].

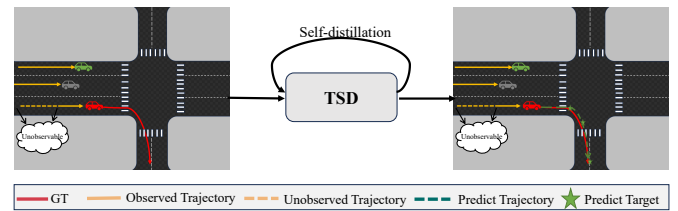


Figure 1: Enhancing the robustness of the model to **partially observed trajectory inputs** through TSD. The agent requiring motion forecasting may have parts of historical trajectory occluded and thus unobservable. Through our proposed TSD, the model can adapt to this situation by leveraging predicted targets and self-distillation.

Many carefully designed networks have achieved excellent results in motion forecasting, including recently proposed methods such as HiVT [Zhou *et al.*, 2022], QCNet [Zhou *et al.*, 2023], and SEPT [Lan *et al.*, 2023a], which have performed exceptionally well on large-scale motion forecasting datasets like Argoverse and Argoverse2. Despite their impressive performance, most open-source large-scale motion forecasting datasets contain carefully collected agent motion data, where the agents typically have complete input and output observations. However, in real-world situations, traffic safety is often compromised due to insufficient observations. For example, obstacles or other agents on the road can obscure parts of the agents, leading to incomplete observations when they appear, which in turn results in erroneous trajectory predictions and affects the safety of autonomous driving systems.

Some methods [Xu and Fu, 2024; Sun *et al.*, 2022] have designed specific networks to address the challenges of partial observation. However, if the goal is to retain the knowledge of the state-of-the-art network trained on fully observed data, many approaches adopt knowledge distillation [Monti *et al.*, 2022; Wang *et al.*, 2024]. Specifically, a network is first trained on fully observed data, and then the knowledge from this network is distilled into an identical network that receives only partially observed inputs. While the network obtained through knowledge distillation retains the original model’s structure and performs well under partial observa-

*Equal contribution.

†Corresponding author.

tion, this approach has two main drawbacks: first, the performance of the distilled network on fully observed data is lower than that of the originally trained network; second, the knowledge distillation process is cumbersome, requiring the training of one network followed by another distillation step, making the entire training process very expensive.

To overcome the aforementioned challenges, as depicted in Figure 1 we propose a novel **Target-driven Self-Distillation** method (**TSD**) for motion forecasting. First, when observations are incomplete, if accurate target points can guide the trajectory prediction process, the model can still make accurate predictions despite the limited observations. Therefore, we propose an anchor-free target point generation method that accurately predicts the target points of agents, thereby guiding accurate trajectory prediction under both partial and full observations. Second, since partially observed trajectories can be viewed as a natural data-distortion branch, we refer to the design for classification tasks in [Xu and Liu, 2019] and develop a self-distillation method for motion forecasting. This method uses fully observed and partially observed inputs as two branches, jointly optimizes these branches, and employs empirical Maximum Mean Discrepancy (MMD) [Long *et al.*, 2015] as a non-parametric metric to measure the consistency of feature distributions between these distorted versions. Through these two aspects, we can obtain a robust model for partial observation data and outperform the vanilla version of the model under full observation with a single end-to-end training process.

Our contributions can be summarized as follows:

(1) We propose **TSD**, a novel plug-and-play method that enhances the robustness of motion forecasting models under partial observation trajectories, and simultaneously improves their motion forecasting capabilities under full observation trajectories.

(2) We design an anchor-free target point generation method based on the Transformer decoder, which iteratively predicts target points over both long-term and short-term time horizons. By accurately predicting target points, this method guides the model in performing precise trajectory prediction under partial observation conditions.

(3) We introduce a new self-distillation mechanism for partially observed trajectories task. This enhances the robustness of the model under partial observation conditions.

(4) Extensive evaluations on multiple large-scale motion forecasting datasets demonstrate that our model not only significantly improves the robustness of baseline models in predicting motion under partial observation but also enhances prediction performance under full observation.

2 Related Works

2.1 Fully Observed Motion Forecasting

Fully Observed Motion Forecasting typically uses complete historical trajectories to predict future motion. Many methods have been proposed in current research, which can be categorized into anchor-based and anchor-free approaches. Methods like [Chai *et al.*, 2019], [Zhao *et al.*, 2021], and [Afshar *et al.*, 2024] cluster representative trajectory anchors as static anchors using unsupervised learning from training data. On

the other hand, [Varadarajan *et al.*, 2022], [Nayakanti *et al.*, 2023], [Shi *et al.*, 2022], and [Ngiam *et al.*, 2022] generate dynamic, learnable anchors through implicit methods. After anchor generation, these methods combine the anchors with contextual information from the scene and use simple networks to predict future trajectories. Anchor-free methods, such as those using diffusion models like [Jiang *et al.*,], [Li *et al.*, 2023], and [Gu *et al.*, 2022], or generative networks like [Barsoum *et al.*, 2018], [Kingma and Welling,], and [Gomez-Gonzalez *et al.*, 2020], rely on the precise capturing of multimodal distributions for prediction. Additionally, some anchor-free methods adopt self-supervised learning approaches, such as [Chen *et al.*, 2023], [Cheng *et al.*, 2023] and [Lan *et al.*, 2023b]. These methods learn more comprehensive scene interaction information by reconstructing features from masked regions and can also achieve impressive trajectory forecasting results. However, these methods, trained on carefully designed datasets with complete trajectory observations, exhibit poor robustness to partially observed trajectory inputs. Their performance typically degrades significantly when encountering those cases.

Our proposed plug-and-play method TSD can significantly enhance the robustness of these approaches when facing partially observed trajectories and also improves their performance under fully observation inputs.

2.2 Partially Observed Motion Forecasting

Partially Observed Motion Forecasting refers to the use of partial historical data for future trajectory prediction. The previously mentioned Fully Observed Motion Forecasting methods tend to give better prediction results only on complete trajectories, but their performance is significantly degraded when partial historical trajectories are masked out, their performance decreases significantly. Numerous works have been proposed to address this issue. Some methods attempt to utilize knowledge distillation to mitigate this problem. [Monti *et al.*, 2022] and [Wang *et al.*, 2024] first train a teacher model on the full trajectory and use this model as the distillation target. Then, they ensure that the feature outputs of the student model, when the input is incomplete, match more closely with those of the teacher model under complete input conditions, thus enhancing performance in the case of trajectory data loss. [Li *et al.*,] introduces a knowledge distillation framework for dynamically varying trajectory lengths and a dynamic neuron soft-masking mechanism to improve the model’s predictive performance when dealing with historical trajectory data of different lengths. Additionally, [Xu and Fu, 2024] learns representations from trajectory data of varying observation lengths and generates time-invariant representations, which are further optimized through an adaptive mechanism, thus improving prediction accuracy. [Li *et al.*, 2023] uses a bidirectional consistency diffusion model to predict future pedestrian trajectories based on short historical trajectory segments. [Sun *et al.*, 2022] proposes a unified feature extractor and a novel pre-training mechanism to capture relevant information in momentary observations, achieving pedestrian trajectory prediction even with extremely short observation lengths. However, these approaches often incur additional training costs and increased model complexity, and

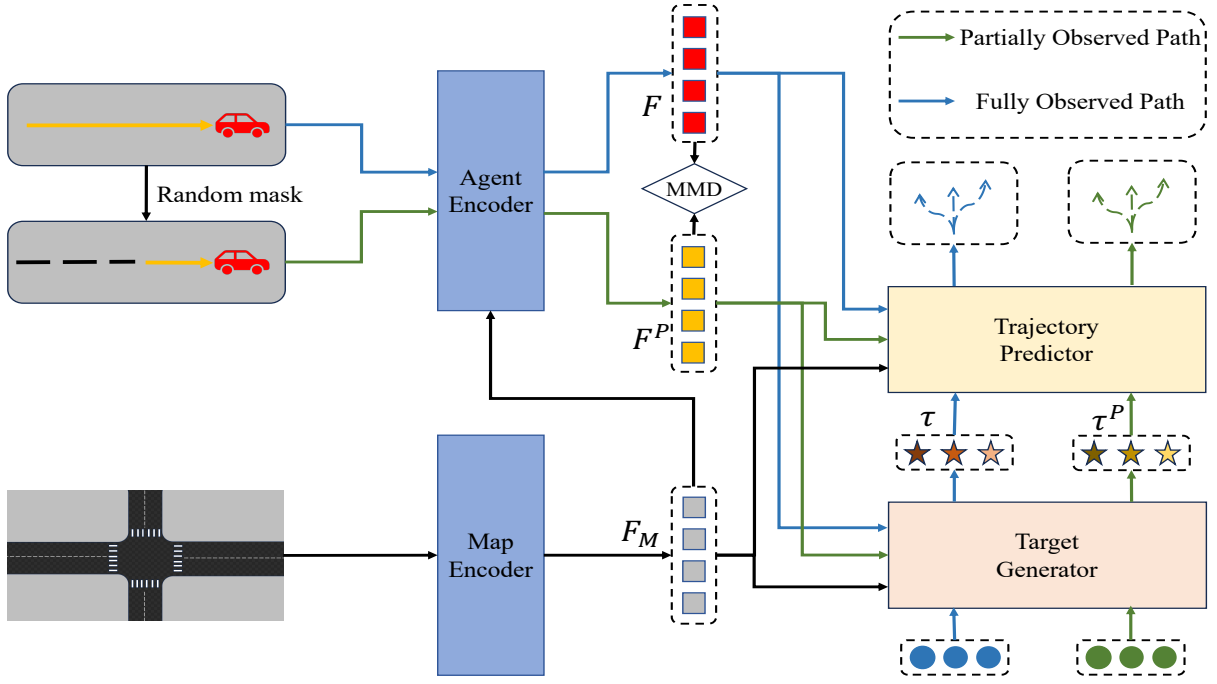


Figure 2: Overview of our proposed TSD. The entire training process is implemented end-to-end. We first apply random masking to the input trajectories to obtain partially observed trajectory branches, which are then fed into the network along with fully observed trajectories. Our proposed target generator produces sequential targets, which subsequently guide the trajectory prediction process. The features extracted from partially observed trajectories and fully observed trajectories are brought closer in distribution using MMD loss. The generation of partially observed trajectories occurs only during training, based on the original fully observed trajectories.

their performance remains poor under extreme missing data conditions.

In contrast, our proposed TSD leverages self-distillation to end-to-end training a model that is robust to partial observation trajectories, and is more efficient and cost-effective.

3 Problem Definition

In the task of motion forecasting, the objective is to predict the future state sequence $X_{\text{pred}} = \{s_t\}_{t=1}^{T_{\text{pred}}}$ of a given agent, based on its past state sequence $X_{\text{obs}} = \{s_t\}_{t=-T_{\text{obs}}+1}^0$, where s_t represents the state of the agent to be predicted at time t . During the prediction, we denote the states of surrounding agents as A , and elements and polylines from the high-definition map provided by the dataset, including lane centerlines, drivable areas, and so on, are denoted as M . Note that the quantities of A and M may not be fixed in a given context. Therefore, our overall objective is to obtain a conditional probability distribution $p(X_{\text{pred}}|X_{\text{obs}}, A, M)$.

Due to the diversity of agents' motion, the conditional probability distribution $p(X_{\text{pred}}|X_{\text{obs}}, A, M)$ can be highly multimodal (*e.g.*, left turn, right turn, going straight, stopping, etc.). By decomposing this task into a target point prediction issue, in the case of predicting trajectories for K modes, the probability distribution can be decomposed as follows:

$$p(X_{\text{pred}}|X_{\text{obs}}, A, M) = \sum_{k=0}^K p(\tau_k|X_{\text{obs}}, A, M) \cdot p(X_{\text{pred}}|X_{\text{obs}}, A, M, \tau_k), \quad (1)$$

where τ_k represents the predicted target point corresponding to the k^{th} mode.

Note that when it comes to partial motion forecasting, the initial observation of past state sequence (X_{obs}) and the agent states (A) are not available at every frame; only a portion of the observations are fed into the model for motion forecasting.

4 Method

4.1 Overview

The overview of our proposed framework is illustrated in Figure 2. We first employ an agent encoder to extract representations of the interested agent and surrounding agents, and a map encoder to extract representations of polylines and elements on the high-definition map. Subsequently, we use a sequential target point generator to iteratively predict long-term and short-term target points for the interested agent over different time horizons. These target points are then used to guide the trajectory predictor to iteratively predict multimodal trajectories. Additionally, during the training phase, we add a partial observation branch. By generating masks, we create partially observed trajectories and feed them into the model along with fully observed trajectories for inference. The inference results from the partially observed trajectories are backpropagated in the same manner as those from fully observed trajectories, and the features extracted from partially observed trajectories are constrained by the features from fully observed trajectories through a loss function.

4.2 Encoder

For motion forecasting, the first step is to use an encoder to embed the trajectory features of each agent and the features of the high-definition map elements, while also exploiting the interactions among agents and map elements. Given X_{obs}, A, M , the encoder outputs the feature embedding $F_X = \{F_{s_t}\}_{t=-T_{\text{obs}}+1}^0 \in \mathbb{R}^{T_{\text{obs}} \times d}$ of the interested agent at historical steps, where d represents the size of the hidden dimension. Additionally, the encoder outputs the features F_A of surrounding agents, the features F_M of map elements, the interaction features $F_{X \rightarrow A}$ between agents and the interaction features $F_{X \rightarrow M}$ between agents and map elements.

4.3 Target Generation and Trajectory Prediction

Here, we propose a target point generation method based on the Transformer [Vaswani *et al.*, 2017] decoder, which can iteratively generate sequential target points over both long-term and short-term time horizons.

Inspired by [Zhou *et al.*, 2023], we assume that the x and y coordinates of target points τ_k^i of the k^{th} mode to be predicted, where $i \in \{1, 2, \dots, n\}$, follow a Laplace distribution, denoted as $\tau_{k,x}^i, \tau_{k,y}^i \sim \mathcal{L}(\mu, b)$. Here, n is the number of target points we set artificially for long-time horizon generation. Therefore, in our target point generation, the ultimate goal is to predict the parameters $\mu_{k,x}^i, \mu_{k,y}^i$ and $b_{k,x}^i, b_{k,y}^i$ for the x and y coordinates of each target point of every mode. Given the multimodal prediction of trajectories for K modes, we generate n target points for each mode; thus, the final set of target points generated for each agent is $\tau \in \mathbb{R}^{K \times n \times 4}$. For the dimension n , target points are generated sequentially over n cycles, each time using the information gathered so far, rather than through an auto-regressive process. Eventually, we can concatenate them as a sequence.

To achieve this, we employed three cross-attention blocks, allowing the target queries to interact and exchange information with the map features, surrounding agents' features, and the historical features of the interested agent. During the information exchange with each type of feature, we also separately utilized the interaction features between the interested agent and the map, surrounding agents, denoted as $F_{X \rightarrow M}$ and $F_{X \rightarrow A}$, as well as the interaction features between different time points of the interested agent, denoted as $F_{s_i \rightarrow s_j}$, where $i, j \in \{T_{\text{obs}}+1, \dots, -1, 0\}$.

Subsequently, we employ two three-layer Feed-Forward Neural Networks (FFNs) to separately deduce the parameters $\mu_{k,x}, \mu_{k,y}$ and $b_{k,x}, b_{k,y}$ of the Laplace distribution for the x and y coordinates of each target points' mode. Based on the predetermined number of target points N , in each iteration, the predicted target point is positioned relative to the previously predicted target point or the starting point, at a future time step of T_{pred}/N . To optimize our target point predictions, we utilize the negative log-likelihood of the Laplace

distribution:

$$\begin{aligned} \mathcal{L}_{\text{tar}} &= \sum_{i=1}^N \sum_{j \in \{x,y\}} \sum_{k=1}^K -\log(\mathcal{L}(s_{\tau_i}; \mu_{k,j}^i, b_{k,j}^i)) \\ &= \sum_{i=1}^N \sum_{j \in \{x,y\}} \sum_{k=1}^K \left(\log(2b_{k,j}^i) + \frac{|s_{\tau_i} - \mu_{k,j}^i|}{b_{k,j}^i} \right), \end{aligned} \quad (2)$$

where s_{τ_i} represents the actual state of the agent at the time step corresponding to the i^{th} generated target point, and

$$\mathcal{L}(s_{\tau_i}; \mu_{k,j}^i, b_{k,j}^i) = \frac{1}{2b_{k,j}^i} \exp\left(-\frac{|s_{\tau_i} - \mu_{k,j}^i|}{b_{k,j}^i}\right). \quad (3)$$

Once obtaining embeddings of the target point e_{τ} , we use them to guide the prediction of future trajectories. For each target point embedding e_{τ_i} , where $i \in \{1, 2, \dots, n\}$, it will guide the trajectory prediction from its previous target point or starting point to the time step corresponding to that target point embedding, with a length of T_{pred}/N .

Similar to target point generation, we set K trajectory queries for each agent, which correspond to the target embeddings derived from each target point query. The trajectory queries first interact with map features, agent features, and historical trajectory features using the cross-attention module, and then we feed them into a multi-head attention module. The query, key, and value are computed as follows:

$$Q = W_q(e_T + e_{\tau_i}), \quad K = W_k(e_T + e_{\tau_i}), \quad V = W_v e_T,$$

where e_T is the embedding of the trajectory query. Finally, we perform self-attention interactions among different modes of the same agent. We also treat the x and y coordinates of each step of an agent's trajectory as following a Laplace distribution like the target point generation, and decode the location and scale of the future trajectory using two FFNs. This process will be repeated N times to generate the complete predicted trajectory. Then, we use a mixture factor π to assign probabilities to each predicted trajectory mode.

We employ two loss functions to optimize the trajectory prediction and the mixture coefficients. For the optimization of trajectory prediction, the loss function is similar to that of Equation 2, with the difference being that it calculates the result of each step in trajectory prediction. We denote this loss as \mathcal{L}_{reg} . During the optimization of the mixture coefficients, the position and scale of the trajectory are detached from the computational graph, focusing solely on optimizing the mixture coefficients:

$$\mathcal{L}_{\text{cls}} = -\log\left(\sum_{k=1}^K \pi_k \sum_{i=1}^{T_{\text{pred}}} \left(-\log(2b_{k,i}) + \frac{|s_{k,i} - \mu_{k,i}|}{b_{k,i}}\right)\right), \quad (4)$$

where K represents the total number of modes to be predicted, and π_k is the probability score assigned to the k^{th} mode.

4.4 Self-Distillation

To end-to-end train a model that is robust to partially observed trajectory inputs, we have designed a self-distillation

Method	b - minFDE ₆ ↓	minADE ₆ ↓	minFDE ₆ ↓	MR ₆ ↓	minADE ₁ ↓	minFDE ₁ ↓	MR ₁ ↓
THOMAS [Gilles <i>et al.</i> , 2022]	2.16	0.88	1.51	0.20	1.95	4.71	0.64
GoRela [Cui <i>et al.</i> , 2023]	2.01	0.76	1.48	0.22	1.82	4.62	0.61
HPTR [Zhang <i>et al.</i> , 2023]	2.03	0.73	1.43	0.19	1.84	4.61	0.61
MTR++ [†] [Shi <i>et al.</i> , 2023]	1.88	0.71	1.37	0.14	1.64	4.12	<u>0.56</u>
MacFormer [†] [Feng <i>et al.</i> , 2023]	1.90	0.70	1.38	0.19	1.84	4.69	0.61
Gnet [†] [Gao <i>et al.</i> , 2023]	1.90	0.69	1.34	0.18	1.72	4.40	0.59
Forecast-MAE [†] [Cheng <i>et al.</i> , 2023]	1.91	0.69	1.34	0.17	1.66	4.15	0.59
ProphNet [Wang <i>et al.</i> , 2023b]	1.88	0.66	1.32	0.18	1.76	4.77	0.61
GANet [†] [Wang <i>et al.</i> , 2023a]	<u>1.81</u>	<u>0.62</u>	<u>1.19</u>	0.14	1.64	<u>4.09</u>	0.55
QCNet [†] [Zhou <i>et al.</i> , 2023]	1.78	<u>0.62</u>	<u>1.19</u>	0.14	1.56	3.96	0.55
TSD-Q (w/o ensemble)	1.87	0.63	1.25	<u>0.15</u>	1.68	4.33	0.58
TSD-Q (w/ ensemble)	1.78	0.61	1.17	0.14	<u>1.59</u>	4.10	<u>0.56</u>

Table 1: Quantitative prediction results on the Argoverse2 motion forecasting benchmark [Wilson *et al.*, 2021], sorted by minADE₆. Baselines known to have used ensembling are marked with the symbol “†”. The best results in each metric are highlighted in **bold**, and the second-best results are underlined.

dim.	Method	Obs. = 1	Obs. = 5	Obs. = 10	Obs. = 15	Obs. = 20
64	HiVT [Zhou <i>et al.</i> , 2022]	1.120/1.761/0.253	0.774/1.168/0.132	0.720/1.085/0.114	0.703/1.061/0.108	0.687/1.030/0.102
	POP-H [Wang <i>et al.</i> , 2024]	1.228/1.857/0.227	0.742/1.117/0.118	0.704/1.060/0.107	0.692/1.040/0.104	0.693/1.043/0.103
	TSD-H	1.040/1.600/0.211	0.739/1.098/0.117	0.694/1.031/0.104	0.679/1.009/0.098	0.675/0.998/0.096
128	HiVT [Zhou <i>et al.</i> , 2022]	1.056/1.652/0.231	0.742/1.098/0.116	0.693/1.023/0.101	0.681/1.005/0.098	0.661/0.969/0.092
	TSD-H	1.002/1.516/0.191	0.716/1.041/0.104	0.671/0.978/0.094	0.657/0.952/0.089	0.653/0.944/0.088

Table 2: Comparison the minADE₆/minFDE₆/MR₆ performance of TSD-H, POP-H, and HiVT under partial observation trajectory inputs, conducted on the Argoverse motion forecasting dataset. For each hidden dimension, the best results are highlighted in **bold**.

method specifically for the motion prediction task. The detailed process of this method is as follows:

(1) The input trajectory data are divided into two branches: complete observations and partial observations. The partially observed trajectory data are obtained by applying random masking to the data X_{obs} and A from the complete observation branch.

(2) Both the complete and partially observed data are fed into the motion prediction network to obtain the intermediate output features and the final prediction results.

(3) For the representation vectors of the intermediate features, we use Maximum Mean Discrepancy (MMD) [Long *et al.*, 2015] to reduce the differences between them. To match the feature distributions, a metric between the representation vectors of the two-branch distorted versions needs to be defined. We adopt the empirical MMD [Long *et al.*, 2015] as a non-parametric metric that has been widely used in domain adaptation to measure the discrepancy of distributions. We use the following empirical MMD loss to minimize the margin between the feature distribution obtained by full observation trajectories ($p(F_A), p(F_X)$ and $p(F_{X \rightarrow A})$) with feature distribution obtained by partial observation trajectories ($p(F_A^P), p(F_X^P)$ and $p(F_{X \rightarrow A}^P)$):

$$\mathcal{L}_{\text{MMD}} = \left\| \frac{1}{n} \sum_{i=1}^n \text{Concat}(F_{X_i}, F_{A_i}, F_{X \rightarrow A_i}) - \frac{1}{n} \sum_{i=1}^n \text{Concat}(F_{X_i}^P, F_{A_i}^P, F_{X \rightarrow A_i}^P) \right\|_2^2, \quad (5)$$

where n denotes the number of total features, F_A, F_A^P denote features of surrounded agents, F_X, F_X^P are features of the interested agent, and $F_{X \rightarrow A}, F_{X \rightarrow A}^P$ are the interaction features between the interested agent and surrounded agents.

(4) For both the complete and partially observed prediction results, the aforementioned $\mathcal{L}_{tar}, \mathcal{L}_{reg}$ and \mathcal{L}_{cls} are used for optimization.

Compared to the training of standard baseline networks, self-distillation training does not add any additional network parameters.

4.5 Training and Inference

We propose that the self-distillation process is only used during training. Specifically, during the training process, we adopt a winner-takes-all training strategy [Lee *et al.*, 2016]. We select the trajectory with the best final target point prediction result from the complete observation for back-propagation and choose the trajectory with the same index from the partial observation output results. Overall, we denote loss for the full observation input branch as $\mathcal{L}_{ful} = \mathcal{L}_{tar} + \mathcal{L}_{reg} + \mathcal{L}_{cls}$, and the loss for the partial trajectory input branch is denoted as $\mathcal{L}_{par} = \mathcal{L}_{tar} + \mathcal{L}_{reg} + \mathcal{L}_{cls}$. Our overall training loss is as follows:

$$\mathcal{L} = \mathcal{L}_{ful} + \mathcal{L}_{par} + \mathcal{L}_{\text{MMD}} \quad (6)$$

5 Experiments

5.1 Experiment Settings

Dataset. We evaluated our proposed model on the Argoverse1 [Chang *et al.*, 2019] and Argoverse2 [Wilson *et al.*, 2021] motion forecasting datasets. The Argoverse1 dataset provides agent trajectories and high-definition map data, containing 323,557 real driving scenarios divided into training, validation, and test sets with 205,942, 39,472, and 78,143 samples, respectively. All training and validation scenes consist of 5-second sequences sampled at 10 Hz, while the test set only reveals the first 2 seconds of the trajectories. Based

Target	SD	Obs. = 1	Obs. = 5	Obs. = 10	Obs. = 15	Obs. = 20
		1.120/1.761/0.253	0.774/1.168/0.132	0.720/1.085/0.114	0.703/1.061/0.108	0.687/1.030/0.102
✓		1.089/1.706/0.248	0.754/1.130/0.124	0.711/1.065/0.109	0.696/1.041/0.103	0.677/1.002/0.099
✓	✓	1.040/1.600/0.211	0.739/1.098/0.117	0.694/1.031/0.104	0.679/1.009/0.098	0.675/0.998/0.096

Table 3: Comparison of the $\min\text{ADE}_6/\min\text{FDE}_6/\text{MR}_6$ performance of different ablation versions of TSD-H. The best results are highlighted in **bold**.

two-branch	MMD	Obs. = 1	Obs. = 5	Obs. = 10	Obs. = 15	Obs. = 20
		1.050/1.625/0.218	0.754/1.130/0.124	0.711/1.065/0.109	0.696/1.041/0.103	0.677/1.002/0.099
✓		1.089/1.706/0.248	0.740/1.106/0.118	0.696/1.040/0.105	0.681/1.014/0.100	0.677/1.005/0.098
✓	✓	1.040/1.600/0.211	0.739/1.098/0.117	0.694/1.031/0.104	0.679/1.009/0.098	0.675/0.998/0.096

Table 4: Comparison of the $\min\text{ADE}_6/\min\text{FDE}_6/\text{MR}_6$ performance of different ablation versions of self-distillation part of TSD-H. The best results are highlighted in **bold**.

on the initial 2 seconds of observation, the model is required to predict the agent’s movement over the next 3 seconds. The Argoverse2 dataset provides agent trajectory data sampled at 10Hz for up to 11 seconds. The training, validation, and test sets contain 199,908, 24,988, and 24,984 samples. Each sample includes the trajectory of the agent to be predicted, and the trajectories of surrounding agents, and comes with high-definition map information of the scene. The objective of the Argoverse2 motion forecasting challenge is to predict the interested agent’s future trajectory for the next 6 seconds based on its trajectory in the previous 5 seconds.

Metrics. We adopted evaluation metrics commonly used in previously state-of-the-art methods [Zhou *et al.*, 2023; Wang *et al.*, 2023b; Wang *et al.*, 2023a; Feng *et al.*, 2023], *i.e.*, minimum Average Displacement Error ($\min\text{ADE}_K$), minimum Final Displacement Error ($\min\text{FDE}_K$), Brier-minimum Final Displacement Error ($\mathbf{b}\text{-minFDE}_K$), and Miss Rate (MR_K). The $\min\text{ADE}$ evaluates the L_2 distance between the coordinates of each step of the top K best-predicted future trajectories by the model and the ground truth, averaged over all time steps. The $\min\text{FDE}$ evaluates the accuracy of the last point’s predicted coordinates. To better gauge the accuracy of uncertainty predictions, $\mathbf{b}\text{-minFDE}$ introduces a weighting factor $(1 - \hat{\pi})^2$ to FDE, where $\hat{\pi}$ represents the probability score allocated by the model to the best-predicted result. The MR metric evaluates the percentage of predictions in $\min\text{FDE}$ that exceed 2 meters. Typically, K is set to 1 and 6. Only the top K predicted trajectories are evaluated if the model outputs more than K trajectories.

Implement Details. We trained HiVT and QCNet integrated with our method (hereinafter referred to as HiVT and QCNet) using the PyTorch deep learning library [Paszke *et al.*, 2019] on 8 RTX 3090 GPUs. The training process included 64 epochs and utilized the AdamW optimizer [Loshchilov and Hutter, 2018]. The batch size for HiVT was set to 32, while it was set to 16 for QCNet due to memory constraints. The initial learning rate, weight decay, and dropout rate for HiVT were set to $3\text{e-}4$, $1\text{e-}4$, and 0.1, respectively; for QCNet, the initial learning rate was set to $5\text{e-}4$, the weight decay to $1\text{e-}4$, and the dropout rate to 0.1. Both models were trained using a cosine annealing scheduler [Loshchilov and Hutter, 2016] to adjust the learning rate. The architecture of HiVT consists of 1 layer of agent-agent and agent-lane interaction

modules, 4 layers of temporal learning modules, and 3 layers of global interaction modules. For QCNet, the number of cross-attention and self-attention layers was set to 2, the MLP contains 3 layers, and the hidden dimension size is set to 128.

5.2 Quantitative Comparisons

Overall Performance with State-of-the-Art. We compare the proposed model with state-of-the-art motion forecasting models on the Argoverse2 motion forecasting dataset [Wilson *et al.*, 2021]. As shown in Table 1, the results indicate that the proposed model exhibits superior performance compared to state-of-the-art methods such as GANet [Wang *et al.*, 2023a], QCNet [Zhou *et al.*, 2023], MacFormer [Feng *et al.*, 2023], Gnet [Gao *et al.*, 2023], ProphNet [Wang *et al.*, 2023b], and ForecastMAE [Cheng *et al.*, 2023]. In the ensemble version of TSD-Q, we employed a simple bagging [Breiman, 1996] ensemble learning technique to enhance the performance of our model by aggregating the predictions from 5 variants of our proposed model (with different numbers of layers, prediction ranges, and random seeds), resulting in trajectories far exceeding the required prediction output. Subsequently, we applied the weighted K-Means [Huang *et al.*, 2005] to cluster these trajectories into the same number of categories as stipulated by the Argoverse 2 motion forecasting challenge (with $K = 6$), adopting the predicted π as the weight. We then calculated the mean of the trajectories within each category to represent the final trajectory of each category.

Robustness with State-of-the-Art. On the Argoverse 1 dataset, we compared the robustness of state-of-the-art models under partial observation trajectory inputs. As shown in Figure 1, we built TSD-H based on HiVT and compared it with HiVT and the state-of-the-art distillation-based method, POP, under different hidden dimension settings. The results indicate that when the input is partial observation data, the performance of HiVT significantly deteriorates regardless of whether the hidden dimension is 64 or 128. Although POP-H can improve model performance under partial observations, it degrades performance under full observations. In contrast, our proposed TSD-H not only significantly enhances the model’s robustness under partial observations at hidden dimensions of 64 or 128 but also maintains or even improves performance under full observations.

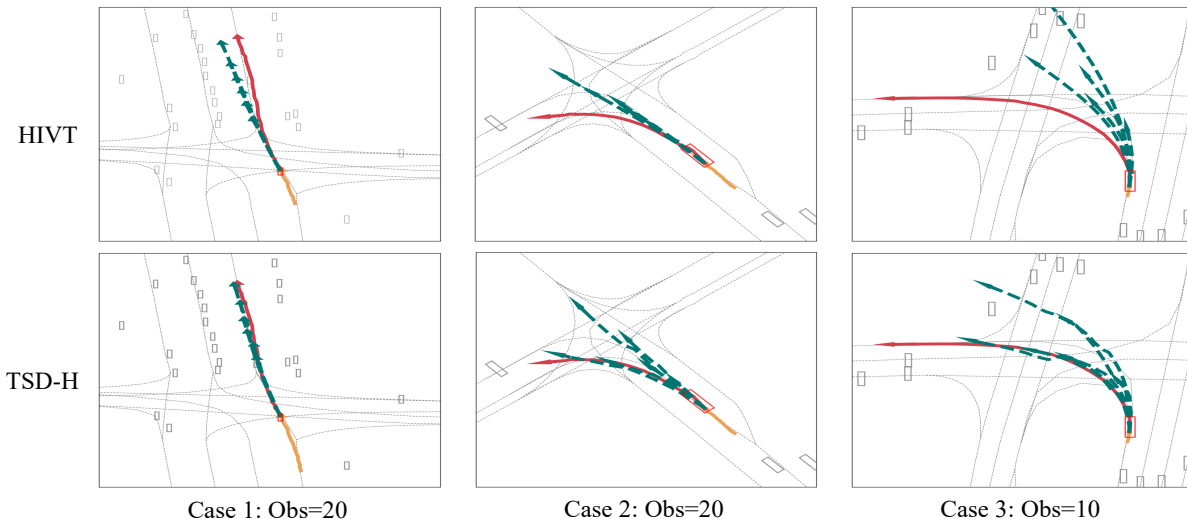


Figure 3: Qualitative results of HiVT and TSD-H. The past trajectories are shown in yellow, the ground-truth trajectories are shown in red, and the predicted trajectories are shown in green. The white boxes are other vehicles around, and the red boxes are agents

5.3 Ablation Studies

Component Ablation. In Table 3, we analyze the gains of each component of the proposed TSD based on TSD-H. The contents of the table show that by predicting accurate proxy target points and performing target-guided trajectory prediction, the model achieves improvements in both fully observed and partially observed trajectories, resulting in an overall performance enhancement. After adding self-distillation to the motion forecasting training, the model shows further improvement in fully observed trajectories and a significant increase in robustness for partially observed trajectory inputs.

Self Distillation Ablation. We also conducted an ablation analysis of the self-distillation component in our proposed method. As shown in Table 4, by adding a branch for partially observed trajectory inputs and using the best mode from fully observed trajectory predictions as the gradient back-propagation mode for partial observations, the model can focus on the prediction results of the best mode under partial observations and perform backpropagation accordingly. After adding the MMD loss, the model further aligns the representations between fully observed and partially observed scenarios, thereby enhancing the model’s robustness and overall performance.

Target Number. We investigate the impact of the number of generated target points on the performance of the proposed model, comparing the results of predictions with six target points, three target points, and a single target point. When testing variants with more than three target points, the number of iterations in the trajectory prediction module is also increased to match the number of target points. As shown in Table 5, when only generating a single long-term target point to guide trajectory generation, the broad time horizon leads to inaccurate target points, significantly impairing the trajectory prediction. When too many target points are predicted, the error accumulation results in less accurate target point generation, slightly reducing trajectory prediction performance.

Targets	Iterations	minADE ₆ ↓	minFDE ₆ ↓	MR ₆ ↓
1	1	0.74	1.33	0.17
1	3	0.74	1.33	0.17
1	6	0.74	1.32	0.17
3	3	0.70	1.24	0.15
3	6	0.70	1.24	0.16
6	6	0.71	1.26	0.16

Table 5: Comparison of the impact of different numbers of target points and the number of iterations for predicting trajectories on the final performance of the proposed model. We investigated as many combinations as possible to prove that our chosen target points and the number of rounds for trajectory prediction are optimal.

5.4 Qualitative Results

To demonstrate the effectiveness of our method, we conducted qualitative experiments on the Argoverse1 dataset, as shown in 3. Case 1 shows a straight-driving scenario with an input history length of 20. Case 2 shows a turning scenario with an input history length of 20. It can be observed that our method, TSD, outperforms the original HiVT in both scenarios. In Case 1, the predicted trajectory of our method is closer to the ground truth than HiVT’s prediction. In Case 2, HiVT incorrectly predicts a straight path, while our method successfully predicts the turning scenario. Case 3 shows an experiment where only part of the historical trajectory is provided, with a history length of 10. In this case, our method predicts the turning trajectory more closely to the ground truth compared to the original HiVT.

6 Conclusion

This paper presented a self-distillation motion forecasting method based on anchor-free target point guidance, tailored to the characteristics of partial observation trajectory prediction tasks. First, the method predicted accurate long-term and short-term target points for different time horizons, which

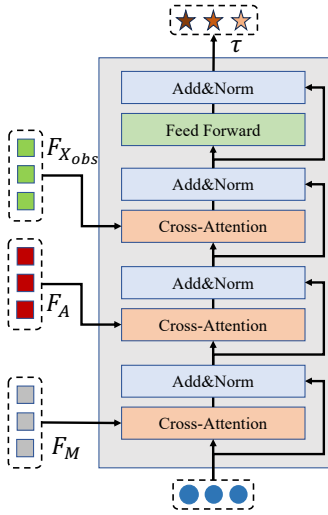


Figure 4: Sequential target generator.

guided precise trajectory prediction under partial observation conditions. Second, we designed a self-distillation approach for partial observation trajectories, ensuring that the feature distributions and prediction results are consistent between full and partial observation scenarios. Extensive experiments demonstrate that the trained model can achieve more accurate motion forecastings under partial observation and also improve prediction performance under full observation.

A Target Generator

Figure 4 illustrates the internal structure of the proposed sequential target generator. This generator is based on the Transformer [Vaswani *et al.*, 2017] decoder architecture, utilizing cross-attention mechanisms to enable interaction between the query and both road features and agent trajectory features. The final predictions for long-term and short-term target points are produced through feed-forward layer.

B Loss Computation

BT	\mathcal{L}_{cls} with T-NLL	minADE ₆ ↓	minFDE ₆ ↓	MR ₆ ↓
		0.73	1.31	0.17
	✓	0.72	1.28	0.16
✓		0.71	1.25	0.16
✓	✓	0.70	1.24	0.15

Table 6: Comparison of the impact of different gradient backpropagation strategies and training losses on the performance of the proposed model. **BT** denote choose the mode with best target prediction as the best mode. \mathcal{L}_{cls} with T-NLL refers to calculating \mathcal{L}_{cls} based on the negative log-likelihood loss of trajectory.

We investigate the impact of different gradient backpropagation strategies and different loss functions for the mixture factor π on the prediction accuracy of target points and the overall performance of motion forecasting, respectively. In the winner-takes-all training strategy, we choose the mode with the best target point prediction for gradient backpropagation and explore the impact of selecting the mode with the

best trajectory prediction. For the mixture factor π , as per \mathcal{L}_{cls} , its objective function is constructed based on the negative log-likelihood loss of the trajectory. To explore the impact of different objective functions, we test constructing \mathcal{L}_{cls} based on the negative log-likelihood loss of the target points.

As shown in Table 6, selecting the mode with the best prediction of target points for gradient backpropagation significantly enhances the accuracy of target point prediction. This allows the model to generate target points more accurately with the corresponding trajectories. Moreover, using the loss function \mathcal{L}_{cls} also improves the overall performance of the proposed model without significantly affecting the prediction accuracy of target points.

C External Analysis

Effect of KL Divergence. Since the self-distillation for classification tasks in [Xu and Liu, 2019] includes KL loss on the predicted classification results, we also attempted to introduce KL loss between our mode classification results. The results are shown in Table 1. It can be seen that after adding the KL loss, there is a slight decrease in the model’s robustness and overall performance, with improvements in the MR6 metric only for certain observation lengths. We speculate that this is because the addition of KL loss causes the model to focus more on the consistency of the best mode selection under fully observed and partially observed conditions, while reducing its attention to other optimization objectives. In the future, we will explore how to balance various losses and how to compute the loss between fully observed and partially observed predictions more effectively to ensure their consistency.

D Discussion

In the future, we will further explore the self-distillation partial observation motion forecasting method with target point guidance. Regarding target point guidance, we believe that introducing statistical priors of future trajectories can enhance the accuracy of target points when observations are insufficient. In terms of self-distillation, we will investigate how to unify the distributions of predicted trajectories and probabilities between full and partial observation conditions. We hope that these further explorations will enhance the robustness of the model under partial observation and contribute to safer autonomous driving technology.

References

- [Afshar *et al.*, 2024] Sepideh Afshar, Nachiket Deo, Akshay Bhagat, Titas Chakraborty, Yunming Shao, Balarama Raju Buddharaju, Adwait Deshpande, and Henggang Cui. Motion. Pbp: Path-based trajectory prediction for autonomous driving. In *ICRA*, pages 12927–12934. IEEE, 2024.
- [Barsoum *et al.*, 2018] Emad Barsoum, John Kender, and Zicheng Liu. Hp-gan: Probabilistic 3d human motion prediction via gan. In *CVPRW*, pages 1418–1427, 2018.
- [Breiman, 1996] Leo Breiman. Bagging predictors. *Machine learning*, 24:123–140, 1996.

Ablation	Obs. = 1	Obs. = 5	Obs. = 10	Obs. = 15	Obs. = 20
w/ KL Loss	1.047/1.615/0.216	0.740/1.110/ 0.116	0.697/1.044/ 0.103	0.682/1.014/ 0.098	0.678/1.008/0.099
w/o KL Loss	1.040/1.600/0.211	0.739/1.098/0.117	0.694/1.031/0.104	0.679/1.009/0.098	0.675/0.998/0.096

Table 7: Comparison of the $\text{minADE}_6/\text{minFDE}_6/\text{MR}_6$ performance of TSD-H self-distillation with and without the addition of KL Loss. The best results are highlighted in **bold**.

- [Chai *et al.*, 2019] Yuning Chai, Benjamin Sapp, Mayank Bansal, and Dragomir Anguelov. Multipath: Multiple probabilistic anchor trajectory hypotheses for behavior prediction. *arXiv preprint arXiv:1910.05449*, 2019.
- [Chang *et al.*, 2019] Ming-Fang Chang, John Lambert, Pat-sorn Sangkloy, Jagjeet Singh, Slawomir Bak, Andrew Hartnett, De Wang, Peter Carr, Simon Lucey, Deva Ramanan, et al. Argoverse: 3d tracking and forecasting with rich maps. In *CVPR*, pages 8748–8757, 2019.
- [Chen *et al.*, 2019] Changan Chen, Yuejiang Liu, Sven Kreiss, and Alexandre Alahi. Crowd-robot interaction: Crowd-aware robot navigation with attention-based deep reinforcement learning. In *ICRA*, pages 6015–6022. IEEE, 2019.
- [Chen *et al.*, 2023] Hao Chen, Jiase Wang, Kun Shao, Furui Liu, Jianye Hao, Chenyong Guan, Guangyong Chen, and Pheng-Ann Heng. Traj-mae: Masked autoencoders for trajectory prediction. In *ICCV*, pages 8351–8362, 2023.
- [Cheng *et al.*, 2023] Jie Cheng, Xiaodong Mei, and Ming Liu. Forecast-mae: Self-supervised pre-training for motion forecasting with masked autoencoders. In *ICCV*, pages 8679–8689, 2023.
- [Cui *et al.*, 2022] Yutao Cui, Cheng Jiang, Limin Wang, and Gangshan Wu. Mixformer: End-to-end tracking with iterative mixed attention. In *CVPR*, pages 13608–13618, 2022.
- [Cui *et al.*, 2023] Alexander Cui, Sergio Casas, Kelvin Wong, Simon Suo, and Raquel Urtasun. Gorela: Go relative for viewpoint-invariant motion forecasting. In *ICRA*, pages 7801–7807. IEEE, 2023.
- [Feng *et al.*, 2023] Chen Feng, Hangning Zhou, Huadong Lin, Zhigang Zhang, Ziyao Xu, Chi Zhang, Boyu Zhou, and Shaojie Shen. Macformer: Map-agent coupled transformer for real-time and robust trajectory prediction. *IEEE Robotics and Automation Letters*, 2023.
- [Gao *et al.*, 2023] Xing Gao, Xiaogang Jia, Yikang Li, and Hongkai Xiong. Dynamic scenario representation learning for motion forecasting with heterogeneous graph convolutional recurrent networks. *IEEE Robotics and Automation Letters*, 8(5):2946–2953, 2023.
- [Gilles *et al.*, 2022] Thomas Gilles, Stefano Sabatini, Dzmitry Tsishkou, Bogdan Stanciulescu, and Fabien Moutarde. Thomas: Trajectory heatmap output with learned multi-agent sampling. In *ICLR*, 2022.
- [Gomez-Gonzalez *et al.*, 2020] Sebastian Gomez-Gonzalez, Sergey Prokudin, Bernhard Schölkopf, and Jan Peters. Real time trajectory prediction using deep conditional generative models. *IEEE Robotics and Automation Letters*, 5(2):970–976, 2020.
- [Gu *et al.*, 2022] Tianpei Gu, Guangyi Chen, Junlong Li, Chunze Lin, Yongming Rao, Jie Zhou, and Jiwen Lu. Stochastic trajectory prediction via motion indeterminacy diffusion. In *CVPR*, pages 17113–17122, 2022.
- [Hu *et al.*, 2023] Yihan Hu, Jiazhi Yang, Li Chen, Keyu Li, Chonghao Sima, Xizhou Zhu, Siqi Chai, Senyao Du, Tianwei Lin, Wenhai Wang, et al. Planning-oriented autonomous driving. In *CVPR*, pages 17853–17862, 2023.
- [Huang *et al.*, 2005] Joshua Zhexue Huang, Michael K Ng, Hongqiang Rong, and Zichen Li. Automated variable weighting in k-means type clustering. *TPAMI*, 27(5):657–668, 2005.
- [Huang *et al.*, 2023] Chenguang Huang, Oier Mees, Andy Zeng, and Wolfram Burgard. Visual language maps for robot navigation. In *ICRA*, pages 10608–10615. IEEE, 2023.
- [Jia *et al.*, 2023] Xiaosong Jia, Penghao Wu, Li Chen, Jiangwei Xie, Conghui He, Junchi Yan, and Hongyang Li. Think twice before driving: Towards scalable decoders for end-to-end autonomous driving. In *CVPR*, pages 21983–21994, 2023.
- [Jiang *et al.*,] Chiyu Jiang, Andre Cornman, Cheolho Park, Benjamin Sapp, Yin Zhou, Dragomir Anguelov, et al. Motiondiffuser: Controllable multi-agent motion prediction using diffusion. In *CVPR*, pages=9644–9653, year=2023.
- [Kingma and Welling,] Diederik P Kingma and Max Welling. Auto-encoding variational {Bayes}. In *ICLR*.
- [Lan *et al.*, 2023a] Zhiqian Lan, Yuxuan Jiang, Yao Mu, Chen Chen, and Shengbo Eben Li. Sept: Towards efficient scene representation learning for motion prediction. In *The Twelfth International Conference on Learning Representations*, 2023.
- [Lan *et al.*, 2023b] Zhiqian Lan, Yuxuan Jiang, Yao Mu, Chen Chen, and Shengbo Eben Li. Sept: Towards efficient scene representation learning for motion prediction. In *ICLR*, 2023.
- [Lee *et al.*, 2016] Stefan Lee, Senthil Purushwalkam Shiva Prakash, Michael Cogswell, Viresh Ranjan, David Crandall, and Dhruv Batra. Stochastic multiple choice learning for training diverse deep ensembles. *NeurIPS*, 29, 2016.
- [Li *et al.*,] Yuhang Li, Changsheng Li, Ruilin Lv, Rongqing Li, Ye Yuan, and Guoren Wang. Lakd: Length-agnostic knowledge distillation for trajectory prediction with any length observations. In *NeurIPS*.
- [Li *et al.*, 2023] Rongqing Li, Changsheng Li, Dongchun Ren, Guangyi Chen, Ye Yuan, and Guoren Wang. Bcdiff:

- Bidirectional consistent diffusion for instantaneous trajectory prediction. *NeurIPS*, 36:14400–14413, 2023.
- [Long *et al.*, 2015] Mingsheng Long, Yue Cao, Jianmin Wang, and Michael Jordan. Learning transferable features with deep adaptation networks. In *International conference on machine learning*, pages 97–105. PMLR, 2015.
- [Loshchilov and Hutter, 2016] Ilya Loshchilov and Frank Hutter. Sgdr: Stochastic gradient descent with warm restarts. In *ICLR*, 2016.
- [Loshchilov and Hutter, 2018] Ilya Loshchilov and Frank Hutter. Decoupled weight decay regularization. In *ICLR*, 2018.
- [Monti *et al.*, 2022] Alessio Monti, Angelo Porrello, Simone Calderara, Pasquale Coscia, Lamberto Ballan, and Rita Cucchiara. How many observations are enough? knowledge distillation for trajectory forecasting. In *Proceedings of the IEEE/CVF Conference on Computer Vision and Pattern Recognition*, pages 6553–6562, 2022.
- [Nayakanti *et al.*, 2023] Nigamaa Nayakanti, Rami Al-Rfou, Aurick Zhou, Krathar Goel, Khaled S Refaat, and Benjamin Sapp. Wayformer: Motion forecasting via simple & efficient attention networks. In *2023 IEEE International Conference on Robotics and Automation (ICRA)*, pages 2980–2987. IEEE, 2023.
- [Ngiam *et al.*, 2022] Jiquan Ngiam, Benjamin Caine, Vijay Vasudevan, Zhengdong Zhang, Hao-Tien Lewis Chiang, Jeffrey Ling, Rebecca Roelofs, Alex Bewley, Chenxi Liu, Ashish Venugopal, David Weiss, Ben Sapp, Zhifeng Chen, and Jonathon Shlens. Scene transformer: A unified architecture for predicting multiple agent trajectories, 2022.
- [Paszke *et al.*, 2019] Adam Paszke, Sam Gross, Francisco Massa, Adam Lerer, James Bradbury, Gregory Chanan, Trevor Killeen, Zeming Lin, Natalia Gimelshein, Luca Antiga, et al. Pytorch: An imperative style, high-performance deep learning library. *NeurIPS*, 32, 2019.
- [Shi *et al.*, 2022] Shaoshuai Shi, Li Jiang, Dengxin Dai, and Bernt Schiele. Motion transformer with global intention localization and local movement refinement. *NeurIPS*, 35:6531–6543, 2022.
- [Shi *et al.*, 2023] Shaoshuai Shi, Li Jiang, Dengxin Dai, and Bernt Schiele. Mtr++: Multi-agent motion prediction with symmetric scene modeling and guided intention querying. *arXiv preprint arXiv:2306.17770*, 2023.
- [Sun *et al.*, 2022] Jianhua Sun, Yuxuan Li, Liang Chai, Hao-Shu Fang, Yong-Lu Li, and Cewu Lu. Human trajectory prediction with momentary observation. In *Proceedings of the IEEE/CVF Conference on Computer Vision and Pattern Recognition*, pages 6467–6476, 2022.
- [Varadarajan *et al.*, 2022] Balakrishnan Varadarajan, Ahmed Hefny, Avikalp Srivastava, Khaled S Refaat, Nigamaa Nayakanti, Andre Cornman, Kan Chen, Bertrand Douillard, Chi Pang Lam, Dragomir Anguelov, et al. Multi-path++: Efficient information fusion and trajectory aggregation for behavior prediction. In *2022 International Conference on Robotics and Automation (ICRA)*, pages 7814–7821. IEEE, 2022.
- [Vaswani *et al.*, 2017] Ashish Vaswani, Noam Shazeer, Niki Parmar, Jakob Uszkoreit, Llion Jones, Aidan N Gomez, Łukasz Kaiser, and Illia Polosukhin. Attention is all you need. *NeurIPS*, 30, 2017.
- [Wang *et al.*, 2023a] Mingkun Wang, Xinge Zhu, Changqian Yu, Wei Li, Yuexin Ma, Ruochun Jin, Xiaoguang Ren, Dongchun Ren, Mingxu Wang, and Wenjing Yang. Ganet: Goal area network for motion forecasting. In *ICRA*, pages 1609–1615. IEEE, 2023.
- [Wang *et al.*, 2023b] Xishun Wang, Tong Su, Fang Da, and Xiaodong Yang. Prophnet: Efficient agent-centric motion forecasting with anchor-informed proposals. In *CVPR*, pages 21995–22003, 2023.
- [Wang *et al.*, 2024] Sheng Wang, Yingbing Chen, Jie Cheng, Xiaodong Mei, Ren Xin, Yongkang Song, and Ming Liu. Improving autonomous driving safety with pop: A framework for accurate partially observed trajectory predictions. In *ICRA*, pages 14450–14456. IEEE, 2024.
- [Wilson *et al.*, 2021] Benjamin Wilson, William Qi, Tanmay Agarwal, John Lambert, Jagjeet Singh, Siddhesh Khandelwal, Bowen Pan, Ratnesh Kumar, Andrew Hartnett, Jhony Kaesemodel Pontes, et al. Argoverse 2: Next generation datasets for self-driving perception and forecasting. *NeurIPS Datasets and Benchmarks*, 2021.
- [Wu *et al.*, 2022] Penghao Wu, Xiaosong Jia, Li Chen, Junchi Yan, Hongyang Li, and Yu Qiao. Trajectory-guided control prediction for end-to-end autonomous driving: A simple yet strong baseline. *NeurIPS*, 35:6119–6132, 2022.
- [Xu and Fu, 2024] Yi Xu and Yun Fu. Adapting to length shift: Flexilength network for trajectory prediction. In *Proceedings of the IEEE/CVF Conference on Computer Vision and Pattern Recognition*, pages 15226–15237, 2024.
- [Xu and Liu, 2019] Ting-Bing Xu and Cheng-Lin Liu. Data-distortion guided self-distillation for deep neural networks. In *Proceedings of the AAAI conference on artificial intelligence*, volume 33, pages 5565–5572, 2019.
- [Zhang *et al.*, 2023] Zhejun Zhang, Alexander Liniger, Christos Sakaridis, Fisher Yu, and Luc Van Gool. Real-time motion prediction via heterogeneous polyline transformer with relative pose encoding. In *NeurIPS*, 2023.
- [Zhao *et al.*, 2021] Hang Zhao, Jiyang Gao, Tian Lan, Chen Sun, Ben Sapp, Balakrishnan Varadarajan, Yue Shen, Yi Shen, Yuning Chai, Cordelia Schmid, et al. Tnt: Target-driven trajectory prediction. In *CoRL*, pages 895–904. PMLR, 2021.
- [Zhou *et al.*, 2022] Zikang Zhou, Luyao Ye, Jianping Wang, Kui Wu, and Kejie Lu. Hivt: Hierarchical vector transformer for multi-agent motion prediction. In *CVPR*, pages 8823–8833, 2022.
- [Zhou *et al.*, 2023] Zikang Zhou, Jianping Wang, Yung-Hui Li, and Yu-Kai Huang. Query-centric trajectory prediction. In *CVPR*, pages 17863–17873, 2023.